Nearshore Wave-Induced Current in the Laboratory

Paul Bayle[1(✉)], Jessamy Mol[1], Kai Kang[1], Colin Whittaker[2], Wout Bakker[1], and Ton van den Bremer[1]

[1] Faculty of Civil Engineering and GeoSciences, Delft University of Technology, Stevinweg 1, 2628CN Delft, The Netherlands
p.b.bayle@tudelft.nl
[2] Civil and Environmental Engineering, The University of Auckland, Auckland 1010, New Zealand

Abstract. The study of nearshore wave-induced currents, which play a critical role in marine transport, has motivated numerous laboratory experiments, and yet, the understanding of cross-shore wave-induced currents under controlled laboratory conditions remains incomplete. For the first time, 3D Particle Tracking Velocimetry is applied in a laboratory flume to measure Lagrangian wave-induced currents in front of a slope under five different regular wave conditions. The wave-induced velocity profiles evolve over time, reaching a quasi-equilibrium after approximately one hour. In most cases, the observed profiles do not align with the theoretical Stokes or conduction solutions. The surface drift is consistently smaller than theoretically predicted, and in some cases even negative, indicating the presence of a strong Eulerian-mean return current in the upper portion of the water column. The observed patterns cannot be explained solely by the relative water depth kh and wave steepness ka, leading to the hypothesis that convection processes contribute to these discrepancies. Further investigation of visually observed coherent convective structures, such as vortex trains, will be undertaken.

Keywords: Stokes drift · Wave-induced currents · PTV · Laboratory flume

1 Introduction

In the nearshore zone, extending from the shoreline to a few kilometres offshore, waves propagating at the ocean surface generate currents that play an important role in marine transport. Modeling marine transport in this area is essential for environmental sciences, but it necessitates a thorough understanding of wave-induced currents throughout the water column. Most existing models have been calibrated using laboratory flume experiments, which aimed to investigate the relationship between wave forcing conditions and the resulting current profiles in both deep and intermediate water depths, in front of and over a slope. Despite over forty research studies on this topic, no clear conclusions can be drawn and the understanding of cross-shore wave-induced currents in laboratory conditions (in front of and over a slope) remains incomplete. The Eulerian-mean

C. Coelho et al. (Eds.): CD 2025, COASTALRL 42, pp. 128–134, 2026.
https://doi.org/10.1007/978-3-032-15477-4_21

velocity ($\overline{U_E}$) profile varies significantly across studies; we can distinguish three types of behaviour: a depth-uniform profile [1], a sheared profile [2], and an anti-Stokes profile (*i.e.*, the velocity equals in magnitude but opposite in direction to the Stokes drift [3]). These discrepancies remain unexplained, leading to the development of empirical models that are limited to representing specific conditions tied to particular laboratory experimental set-ups.

A comprehensive literature review of existing experiments does not reveal any new relationships or explanations beyond those already published; however, one potential source of the observed discrepancies can be identified in the measurement methods used. In the shoaling zone, only five out of twenty-three studies recorded Lagrangian velocity, with four of these employing visual techniques (*e.g.*, dye), which are nowadays considered relatively imprecise given the developments in measurement technology. In studies that measured Eulerian velocity, accurate quantification of Eulerian flow has only been performed using point probe measurement techniques, such as Laser Doppler Velocimetry (LDV). As a result, a complete velocity profile is effectively an artificial representation, constructed over time, unless perfect reproducibility is assumed and measurements are taken at the exact same time over multiple repetitions, which is rarely the case. However, with the advancement of new measurement technologies over recent decades, these limitations can be mitigated, significantly enhancing our ability to track particle trajectories accurately and investigate Stokes drift and Eulerian-mean current profiles [4].

In this study, a laboratory experiment is conducted in which, for the first time, 3D Particle Tracking Velocimetry (PTV) is applied to investigate wave-induced currents near the shoaling zone. The goal is to compare wave-induced current profile under different hydrodynamic forcing to compare with literature and theoretical solutions.

2 Methodology

The experiment was conducted in the TU Delft Hydraulic Engineering Laboratory, in the 39 m long, 0.79 m wide and 1 m high wave flume. A 1:25 planar slope was installed within the flume to facilitate wave dissipation through breaking (Fig. 1).

Optical access was provided via the glass sidewalls and a bottom glass window positioned one meter offshore of the beach toe. Fluid velocity measurements were obtained using a 3D Particle Tracking Velocimetry (PTV) system from LaVision, which comprises a 'MiniShaker' apparatus (a box containing four fixed-angle cameras capturing images at 100 fps), two LED light boxes, and the 'Shake-the-Box' data processing system. The 3D PTV technique involves illuminating a fluid volume seeded with neutrally buoyant particles and tracking these particles in space and time throughout the measurement volume. Additionally, an overhead camera was positioned 3.30 m above the still-water level to track 4 mm plastic spheres floating on the surface.

A total of five regular wave conditions were tested (Table 1) in multiple repeats. These conditions ensured an intermediate water depth regime at the wave paddle. Each trial had a duration of two hours, during which multiple PTV recordings, each lasting 1 min and 12 s, were acquired consistently at different times. Hundreds of tracks spanning multiple wave periods were extracted, from which the Lagrangian-mean velocity ($\overline{U_L}$)

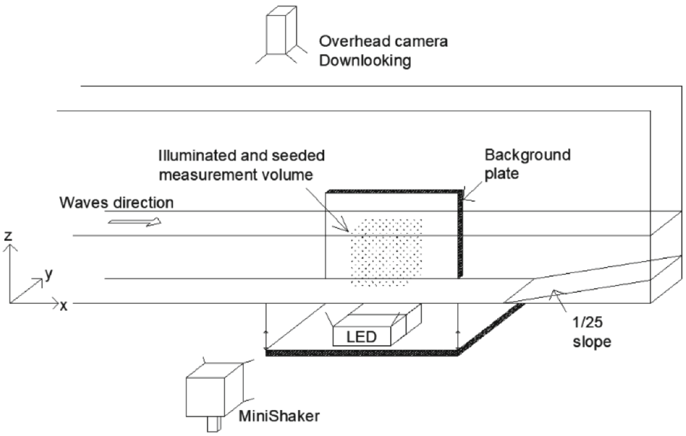

Fig. 1. Experimental set-up. The measurement volume is 50x30x15 cm (length, height, depth).

was computed for each wave, resulting in thousands of velocity data points distributed through the water column. The resulting Lagrangian-mean velocity is space-average over the measurement volume.

$$\overline{U_L} = \overline{U_E} + U_{SD} \quad (1)$$

Table 1. Wave conditions and theoretical Stokes drift (U_{SD}) at the surface ($z = 0$). H is the wave height, T the wave period, ka the wave steepness, kh the relative water depth, Ur the Ursell number and Re the wave Reynolds number. The water depth h = 0.35 m for all conditions.

Wave	H [m]	T [s]	ka [-]	kh [-]	Ur [-]	Re [-]	$U_{SD}(z = 0)$ [cm/s]
W1	0.10	1.80	0.10	0.71	22	12500	3.3
W2	0.13	1.40	0.18	0.96	16	22300	7.3
W3	0.06	1.20	0.10	1.18	5	5000	2.0
W4	0.07	1.40	0.09	0.96	8	6500	2.1
W5	0.04	0.85	0.11	2.02	1.1	711	1.8

Note that the Lagrangian-mean velocity ($\overline{U_L}$, , where the overbar means 'wave-averaged') of a fluid parcel is the sum of the Stokes drift (U_{SD}) and the Eulerian-mean velocity ($\overline{U_E}$) of the fluid measured at a fixed spatial location [5]:

3 Results

3.1 Profile Evolution Over Time

Figure 2 displays the Lagrangian-mean velocity profile over time for wave condition W4. Each blue dot represents a Lagrangian-mean velocity over a single wave period, plotted at the mean elevation z of the tracked particle during that period. The red line indicates the mean velocity as a function of z, with the 95% confidence interval shown as the red shaded area. Note that the high density of points near the mean explains the narrow confidence interval. The surface drift, measured with the overhead camera, is marked by a purple triangle, and the elevation of the wave trough is indicated by the horizontal dashed line. Missing data near the surface and bottom boundaries, due to intense light reflection, are interpolated linearly (dotted lines), though this should be treated as speculative. The theoretical irrotational Stokes and (rotational) conduction solutions [6] are shown as dashed blue and green lines, respectively.

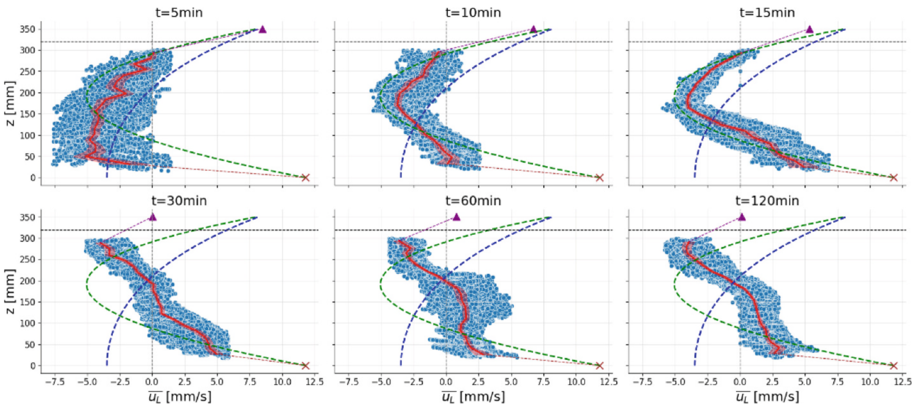

Fig. 2. Lagrangian-mean velocity measurements through the water column for W4 at t = 5, 10, 15, 30, 60 and 120 min after the beginning of wave generation. The legend is shown in Fig. 3.

Figure 2 illustrates the evolution of the velocity profile over time for W4, reaching near-equilibrium after 30 min. While the measured velocity profile closely aligns with the conduction solution at 15 min, it stabilizes at a profile not represented by either theoretical solution. A similar pattern is observed for other wave conditions, with quasi-equilibrium always reached after 60 min. A similar amount of time to reach such quasi-equilibrium was reported by Russell and Osorio [7] and Mei et al. [8], for similar laboratory scales with a beach slope of 1:10 and 1:20, respectively. The surface drift deviates significantly from theory at equilibrium, initially approximating the Stokes solution at t = 5 min but decreasing over time, sometimes becoming negative. Since the Stokes solution is the sum of the Stokes drift and a negative depth-uniform Eulerian-mean 'return' current (to ensure a zero depth-integrated volume flux), the smaller surface drift suggests a sheared Eulerian-mean return current, with maximum magnitude in the upper part of the water column. Only in deeper water, W5 exhibits a surface drift matching the Stokes solution, though the rest of the profile differs notably (Fig. 3).

3.2 Profile as a Function of *kh* and *ka*

Figure 3 compares the profiles at equilibrium for all wave conditions. Comparing wave conditions with similar $ka \approx 0.10$, but different kh (W1, W3, W4 and W5), the conduction solution seems to align with measurements for W1, while neither solution describes measurements for the other wave conditions. This is in contradiction with the literature, from which it can be concluded that the velocity profile tends towards the Stokes solution for $kh > 1.8$, and towards the conduction solution for $0.7 < kh < 1.8$ [7, 8]. It nonetheless seems that the profiles become less and less sheared as kh increases.

For wave conditions W4 and W2, which have the same kh but different ka, both profiles are similarly sheared (albeit with different magnitudes). They both experience a strong Eulerian-mean return current in the upper layer, which significantly reduces the surface drift compared to the Stokes drift (Table 1). We have not considered a large enough number of ka-values to draw general conclusions. Nonetheless, Bijker et al. [9] and Russel and Osorio [7] found that for both small wave steepness (ka) and relative water depth (kh) conditions, the profile gradually changes into a shape where a back flow occurs at the surface. Although a similar trend is observed here, the differences cannot be explained by the influence of the kh and ka alone. Thus, we expect that other processes not accounted for in the Stokes and conduction solution must be involved.

Figure 3 shows that the Lagrangian-mean velocity profile for W3 is very close to zero along the complete vertical, suggesting the Eulerian-mean return current almost cancels out the Stokes drift. This was observed in previously performed lab experiments [3] without providing clear explanation, also lacking data near the bottom boundary layer. These limits drawing clear conclusions, especially as one might expect positive velocity in this area due to the boundary-layer streaming occurring in intermediate water depth [6]. Nonetheless, the three types of behaviour of the Eulerian-mean return profile, as described in Sect. 1, were observed at various points during the experiment.

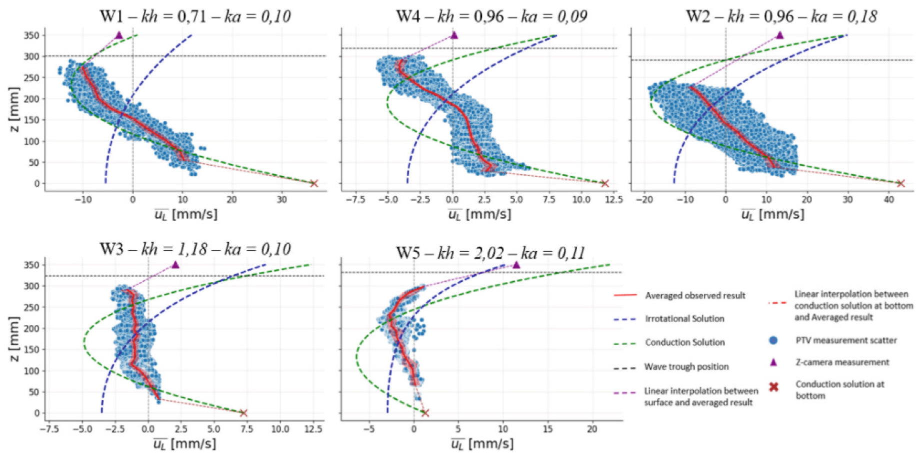

Fig. 3. Lagrangian-mean velocity profile at t = 120 min for all wave conditions. W1, W3, W4 and W5 have a similar wave steepness $ka \approx 0.10$ (Table 1). W2 and W4 have the same $kh = 0.96$.

4 Conclusion

For the first time, 3D Particle Tracking Velocimetry (PTV) was employed to acquire high-resolution wave-induced current velocity profiles in front of a slope, in a laboratory set-up. This direct Lagrangian measurement technique allows for unprecedented spatial and temporal resolution flow measurements, circumventing the technical limitations inherent in Eulerian methods, such as Laser Doppler Velocimetry (LDV). The time required for the velocity profile to reach a quasi-equilibrium state was observed to be 60 min at the experimental scale. Although the equilibrium time has been documented in several studies, it is often overlooked, resulting in the publication of unstable profiles that may contribute to discrepancies in the existing literature. It is critical for laboratory data used in model calibration to be obtained after the equilibrium has reached, as most numerical models generate equilibrium profiles [10].

With the exception of W1, which aligns with the conduction solution at equilibrium, none of the measured profiles correspond to either of the Stokes or conduction theoretical solutions. Note that the conduction solution is theoretically not applicable for steep waves, while the Stokes solution is only valid for deep-water where a bottom boundary layer is absent. The three distinct types of behaviour of the Eulerian-mean return profile were observed at various points during the experiment, suggesting their occurrence may not laboratory dependent. However, contrary to the findings reported in the literature, no straightforward relationship with kh and ka could be established over the range of conditions tested. This indicates that other factors, including processes such as convection, must be considered. Coherent vortex structures, visually observed during the experiment and similar to those described by Matsunaga et al. [11], which are a function of the parameters ka, kh and beach slope, could contribute to some of the observed differences. Further analysis will be conducted to explore these interactions.

References

1. Grue J, Kolaas J (2016) Experimental particle paths and drift velocity in steep waves at finite water depth. J Fluid Mechan 810
2. Dyke PPG, Barstow SF (1981) Wave Induced Mass Transport: Theory And Experiment. J Hydraul Res 19(2):89–106
3. Monismith SG, Cowen EA, Nepf HM, Magnaudet J, Tais L (2007) Laboratory observations of mean flows under surface gravity waves. J Fluid Mech 573:131–147
4. van den Bremer TS, Whittaker C, Calvert R, Raby A, Taylor PH (2019) Experimental study of particle trajectories below deep-water surface gravity wave groups. J Fluid Mech 879:168–186
5. Andrews D, McIntyre M (1978) An exact theory of nonlinear waves on a lagrangian-mean flow. J Fluid Mechan 89: 609–646, 12
6. Longuet-Higgins SM (1953) Mass transport in water waves. Phil Trans Roy Soc London A 245(903): 7611–7618
7. Russell RCH, Osorio JDC (1957) An Experimental Investigation of Drift Profiles in a Closed Channel. Proc VI Conf on Coastal Eng Chap 10:171–193
8. Mei CC, Liu PLF, Carter TG (1972) Mass transport in water waves. Report No. 146, Massachusetts Institute of Technology
9. Bijker EW, Kalwijk JPT, Pieters T (1974) Mass transport in gravity waves on a sloping bottom. Proceedings of the International Conference in Coastal Engineering
10. Larsen BE, Fuhrman DR (2018) On the over-production of turbulence beneath surface waves in Reynolds-averaged Navier-Stokes models. J Fluid Mech 853:419–460
11. Matsunaga N, Takehara K, Awaya Y (1994) The offshore vortex train. J Fluid Mech 276:113–124